Proceedings of the 2002 IEEE
International Conference on Robotics & Automation
Washington, DC • May 2002

A Study on the Sources of Perceptual Instability During Haptic Texture Rendering

Seungmoon Choi and Hong Z. Tan
Haptic Interface Research Laboratory
Purdue University
1285 EE Building, West Lafayette, IN 47907-1285
{*chois, hongtan*}*@purdue.edu*

Abstract

This paper reports the results of our current research towards a qualitative characterization of the instability that a human user often perceives from a virtual textured surface rendered with a force-reflecting haptic interface. Based on our previous study of perceptual instability during haptic texture rendering, an experiment is designed and conducted in order to measure the proximal stimuli delivered by the virtual textures in terms of several physical variables (position, force, and acceleration). The measured data are analyzed in the frequency domain and characterized by sensation levels with regards to the human detection thresholds for temporal stimuli. In particular, a spectral band that conveys texture information and another one that induces instability perception are identified along with their associated sensation levels. These frequency bands excite different mechanoreceptors in the skin, and are therefore perceptually distinctive.

1 Introduction

Haptic texture rendering is a growing research field that holds much promise for enriching the sensory attributes of objects in a virtual environment. It also allows for precise and systematic control of textured surfaces for psychophysical studies. One problem that has become apparent is the perceived instability experienced by human observers while interacting with a virtual textured surface rendered by a haptic interface. Our work has therefore concentrated on the perceptual analysis of such instabilities. Our previous work has produced a quantitative specification of the range of rendering parameters that result in perceptually stable textured surfaces [3, 4]. This paper reports our findings from a follow-up study that investigated the sources of perceptual instability during haptic texture rendering.

Although everyone has some notion of what texture is, the concept of texture is not clearly defined. Katz considered texture as the fine structure of a surface (microstructure), and as independent of the shape (macrostructure) of an object or surface [12]. The systematic study of haptic texture perception began about thirty years ago [22]. Most research has focused on roughness perception. One topic that has been controversial is whether information about surface roughness is encoded *spatially* or *temporally* (with some researchers arguing for the former [5, 6, 16, 21, 30], and Katz for the latter [12]). It is now generally accepted that humans prefer to use intensive (depth of microstructures) and/or spatial (size of microstructures) cues during direct (fingerpad) exploration when both spatial and temporal cues are available [10]; and that humans rely on temporal cues (vibration) during indirect (probe-mediated) exploration when no spatial/intensive cues are available [14, 20]. In addition, roughness perception is very similar whether the direct or the indirect method is employed [18, 19]. There is also evidence that temporal cues are responsible for perception of very fine surface details (with interelement spacing below 1 mm) [9, 11, 15], and that the probe method produces greater perceived roughness than the fingerpad method for very smooth surfaces [13].

It follows that devices that emulate probe-mediated texture exploration should yield successful rendering of textured surfaces, with superior performance expected for very small-scale (less than 1 mm) surface features. Minsky's *Sandpaper* system was perhaps the first successful attempt at generating synthetic textures with a two degree-of-freedom (DoF) force-feedback joystick [24, 25]. Several successful implementations of texture rendering methods using three (or more) DoF force-reflecting devices have also been reported (for examples, see [7, 8, 23, 26, 27]).

To those of us who have felt a textured surface rendered by a haptic interface, it is immediately clear that the perception of texture is often tainted by undesirable *buzzing* and other kinds of *noise* (see, for example, [34, 35]). It is therefore crucial to understand the conditions under which haptically rendered textured surfaces are guaranteed to be perceptually stable. Our previous work focused on the analysis of perceptual instability that occurred when human observers explored virtual textured surfaces with a force-reflecting haptic interface (the PHANToM) [3, 4]. We con-

0-7803-7272-7/02/$17.00 © 2002 IEEE

ducted psychophysical experiments using the method of limits in order to empirically determine the thresholds for the stiffness parameter below which textured virtual surfaces were perceived to be stable. These stability thresholds were assessed under thirty-six experimental conditions where we varied the texture rendering algorithm, exploration mode, and parameters of the surface model (amplitude and wavelength of sinusoidal texture model). Three subjects (one experienced and two naive) participated in the previous experiments.

To our surprise, the maximum stiffness values for perceptually stable textured surfaces were limited to 0.45 N/mm or less. This stiffness range was quite small and corresponded to surfaces that were soft and spongy to the touch. The stiffness thresholds were also dependent on the rendering algorithm, exploration mode and surface model parameters. A simple spring model with a fixed force direction resulted in more perceptually stable surfaces than one with varying force directions based on the local surface normals. Virtual surfaces explored with lateral stroking were perceived to be more stable than those with a free interaction style. The dependency of stiffness thresholds on the surface model parameters was more complex.

Given the relatively limited range of stiffness values that was usable in haptic texture rendering, we decided to turn our attention to the investigation of the sources of perceived instability, and the development of strategies for mitigating this problem. Our current study employs an instrumented force-reflecting device to record the position, force and acceleration signals experienced by a hand during the exploration of virtual textured surfaces. Data are collected for both perceptually stable and unstable renderings. For unstable renderings, we concentrate on three types of perceptual instabilities discovered in our previous study. The first is *entry instability*. As a stylus approaches the textured surface, one sometimes experiences "buzzing" of the stylus. The second type is associated with poking. It is most evident when the stylus is pushed deep into the virtual surface (*inside instability*). These two types of instability are associated with the experimental conditions where subjects were permitted to explore the textured surface in any manner. The third type of instability occurs when a stylus is moved across the textured surface. One sometimes experiences "buzzing" that cannot be attributed to the texture. By analyzing recorded data and comparing our results from perceptually stable and unstable renderings of texture, we hope to discover the signals that give rise to perceived instability during haptic texture rendering.

2 Rendering and Perception of Texture

The texture model, rendering methods, and exploration modes used in this study are the same as those used in our previous study [4]. A brief summary is presented here.

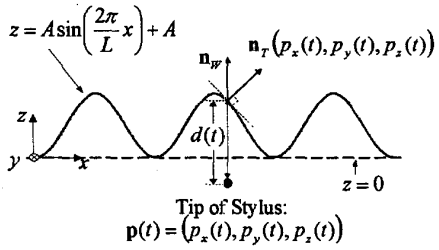

Fig. 1. An illustration of the parameters used in texture rendering. Note that y-axis goes into the plane. See Sec. 2 for details.

The virtual textured surfaces are modeled as one-dimensional sinusoidal gratings superimposed on a flat surface. This underlying flat surface, expressed by $z = 0$ in the world coordinate of PHANToM, forms a vertical wall facing the user of the PHANToM. The sinusoidal gratings are described by $z = h(x, y) = A\sin(\frac{2\pi}{L}x)+A$, where A and L denote the amplitude and (spatial) wavelength, respectively. Sinusoidal gratings are widely used in the haptic texture-rendering literature (for example, see [20, 35]), since surface profiles can be successfully modeled by a Fourier series [33].

Two basic texture rendering methods, both using a spring model to calculate the magnitude of rendered force but differing in the way force directions are rendered, are employed. Force magnitudes are calculated as $K \cdot d(t)$, where K is the stiffness of the textured surface, and $d(t)$ is the penetration depth of the stylus at time t (see Fig. 1). The penetration depth is calculated as

$$d(t) = \begin{cases} 0 & \text{if } p_z(t) > 0 \\ A\sin\left(\frac{2\pi}{L}p_x(t)\right) + A - p_z(t) & \text{if } p_z(t) \le 0 \end{cases}, \quad (1)$$

where $\mathbf{p}(t) = \left(p_x(t), p_y(t), p_z(t)\right)$ is the position of the tip of the stylus.

In terms of force directions, the first method, introduced by Massie [23], renders a force $\mathbf{F}_{mag}(t)$ with a constant direction normal to the underlying flat wall of the textured surface. The second method, proposed by Ho, Basdogan and Srinivasan [8], renders a force $\mathbf{F}_{vec}(t)$ with varying directions such that it remains normal to the local micro-geometry of the sinusoidal texture model. Mathematically,

$$\mathbf{F}_{mag}(t) = K\, d(t)\, \mathbf{n}_W, \quad (2)$$

$$\mathbf{F}_{vec}(t) = K\, d(t)\, \mathbf{n}_T(\mathbf{p}(t)), \quad (3)$$

where $\mathbf{n}_W$ is the normal vector of the underlying flat wall, and $\mathbf{n}_T(\mathbf{p}(t))$ is the normal vector of the textured surface at $\mathbf{p}(t)$ (see Fig. 1). Note that both methods keep the force

vectors in the horizontal planes, thereby minimizing the effect of gravity on rendered forces (See Fig. 2 for the actual orientations of the axes).

Two exploration modes (free exploration and stroking) are tested. In the free exploration mode, subjects are allowed to determine the interaction pattern that is most effective at discovering the instability of the rendered textures and to use that pattern in the experiments. This mode is selected to be the most challenging interaction pattern for a haptic texture rendering system in terms of perceptual stability. With the stroking mode, subjects are instructed to move the stylus laterally across the textured surfaces. This mode is chosen to be representative of the typical and preferred exploration pattern for accurate texture perception [17].

As discussed earlier, a force-reflecting haptic interface such as the PHANToM can only deliver temporal perceptual cues for texture rendering. Hence, it is necessary that a user move the interaction tool of the force-reflecting device across surfaces in order to perceive textures through the resulting temporal cues. In our previous study, when the subjects were allowed to explore textured surfaces freely, they chose to position the PHANToM stylus near the surface boundary or inside the surface to investigate instability. In that case, they were able to detect unrealistic vibration in the absence of other temporal cues that encoded texture. When the subjects used the stroking mode, however, they had to attend to, and separate, the temporal cues that correspond to texture and instability.

To the authors who are experienced with the perceptual qualities of sinusoidal movements across the frequency range of DC to 400 Hz [29], the "buzzing" that contributes to perceived instability during both free exploration and stroking modes seems to be vibrational (i.e., above 100 Hz) in nature. The signals responsible for perceived texture appear to be of lower frequency. The exact frequency of the texture signal can be predicted from our texture model and an estimate of the stroking velocity. Suppose that a human user explores the textured surface by moving the stylus along the x-axis as shown in Fig. 1 with a constant velocity v_x, while maintaining contact with the textured surface. Then, the magnitude of the rendered force can be decomposed into two terms. From Eqns. 2 and 3,

$$\left|\mathbf{F}_{mag}(t)\right| = \left|\mathbf{F}_{vec}(t)\right| = \left|KA\sin\left(2\pi\frac{v_x}{L}t\right) + K\left(A - p_z(t)\right)\right|, \tag{4}$$

assuming that $p_x(0) = 0$. The left term delivers the texture signal at frequency v_x/L, and the right term resists the penetration of a stylus into the textured surface.

In order to understand the nature of the signals that give rise to the perceived instability and texture, we measure the proximal stimuli (position of the tip of the stylus, force, and acceleration) delivered to the subjects during the perception of virtual textures. It follows from the above discussion that we expect to observe high-frequency signal components whenever a virtual textured surface is perceived to be unstable. We also expect to find a signal component at predicted frequency for texture perception during stroking mode. We therefore characterize the data in the frequency domain, with respect to the human detection thresholds at corresponding frequencies.

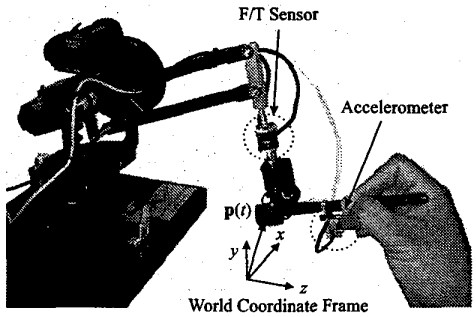

Fig. 2. The PHANToM instrumented with triaxial F/T sensor and accelerometer.

3 Experiment Design

3.1 Apparatus

In the current study, we use a PHANToM force-reflecting device (SensAble Technologies, Woburn, MA; model 1.0A, with a stylus and orientation gimbals) instrumented with two additional sensors (see Fig. 2).

The position of the tip of the stylus, $\mathbf{p}(t)$, is measured using the position sensing routines in the GHOST library provided with the PHANToM. The routines use optical encoders attached at each joint of the PHANToM and convert the joint angles to the position in the world coordinate frame. The resulting nominal resolution is 0.03 mm in the world coordinate frame.

Force delivered by the PHANToM, $\mathbf{f}(t)$, is measured with a triaxial force/torque (F/T) sensor (ATI Industrial Automation, Apex, NC; model Nano17 with temperature compensation). In order to minimize the structural change to the PHANToM, a new link with a built-in interface for the F/T sensor is fabricated to replace the last link (i.e., the link closest to the stylus) of the PHANToM. The new link is of the same length as the original one, and weighed 60 g (13%) more with the F/T sensor. The force sensor has a measurement range of ±12 N with a nominal resolution of 0.0125 N. Force data are transformed into the stylus coordinate frame and recorded. The origin of the stylus coordinate frame is always located at the tip of the stylus (i.e., $\mathbf{p}(t)$), and its z-axis coincides with the cylindrical axis of

Table 1. Experimental conditions.

Condition No.	Exploration Mode	Texture Rendering Method	Perceptual Category	Texture Model Parameters A (mm), L (mm), K (N/mm)
A	Free Exploration	$\mathbf{F}_{mag}(t)$	Entry Instability	1, 2, 0.30
B	Free Exploration	$\mathbf{F}_{vec}(t)$	Entry Instability	1, 2, 0.30
C	Free Exploration	$\mathbf{F}_{vec}(t)$	Inside Instability	1, 2, 0.05
D	Stroking	$\mathbf{F}_{mag}(t)$	Stable	1, 2, 0.15
E	Stroking	$\mathbf{F}_{mag}(t)$	Unstable	1, 2, 0.40
F	Stroking	$\mathbf{F}_{vec}(t)$	Stable	1, 2, 0.15
G	Stroking	$\mathbf{F}_{vec}(t)$	Unstable	1, 2, 0.40

the stylus.

Vibration of the stylus is captured with a triaxial accelerometer (Kistler, Blairsville, PA; model 8794A500). In order not to miss any spectral components, we have selected an accelerometer with a wide range of ±500 G (1 G= 9.8 m/s^2) for all three channels. The accelerometer is attached through a rigid mounter that is press-fitted to the stylus. The attachment adds 11.8 g to the weight of the stylus. Acceleration measurements, $\mathbf{a}(t)$, are also taken in the stylus coordinate frame. With a 12-bit A/D converter, our acceleration data have a nominal resolution of 0.244 G.

3.2 Experimental Conditions

A total of seven experimental conditions are employed as listed in Table 1. In the conditions using the free exploration mode (Conditions A, B, and C), we test perceptually unstable conditions differing in the types of perceived instability: entry and inside instability. Note that inside instability for $\mathbf{F}_{mag}(t)$ is not tested because this type of instability was not observed during our previous study. For the stroking mode, we record data for both perceptually stable (Conditions D and F) and unstable cases (Conditions E and G). Both rendering methods are tested for the stroking mode.

Whether a particular experimental condition results in perceptually stable or unstable rendering also depends on the values of the surface model parameters (A, L, K). The values listed in Table 1 are selected based on the results obtained from our previous study [3, 4].

3.3 Procedures

For the experiments with free exploration mode, subjects are instructed to hold the stylus still near the textured surface (Conditions A and B) or deep inside of it (Condition C). They have to find a point in space where the surface is clearly perceived to be unstable and maintain that position. Once the subject is satisfied with the selected stylus position, the experimenter initiates data collection.

For the experiments with stroking mode (Conditions D, E, F and G), subjects are instructed to move the stylus laterally across the virtual gratings. They are required to maintain a constant stroking speed to the best of their ability. After the subject has initiated stroking, the experimenter starts data collection.

In all experiments, subjects are asked to hold the stylus as if they were holding a pen (see Fig. 2). Three-dimensional position, force and acceleration data are collected for ten seconds at a sampling rate of 1 kHz.

3.4 Subjects

Two subjects participated in the experiment (one female, S1 and one male, S2). Their average age was 33 years old. Both are right-handed and report no known sensory or motor abnormalities with their upper extremities. Only S2 had participated in our previous psychophysical study of perceptual instability.

Both subjects were experienced users of the PHANToM device. They were preferred over naive subjects in the current study, because the subjects had to place or move the stylus in a particular manner in order to maintain well-controlled conditions during data collection. Although we did not expect recorded signals to be significantly different across subjects, we nevertheless took data from two subjects in order to check the consistency and generality of our results.

3.5 Data Analysis

Each ten-second long time-domain signal is processed as follows. Ten spectral densities corresponding to the ten one-second segments of the signal are computed and averaged for noise reduction. We use a flat-top window for precise recovery of the magnitude of each spectral component [28]. The frequency and magnitude of each prominent spectral component are then calculated.

In order to assess the *perceived magnitude* of these spectral peaks, we compare our data to published literature on human detection thresholds of sinusoidal movements. In our experiments, the stylus is in contact with the distal pads of three fingers (thumb, index finger, and middle finger), and the web between the thumb and the index finger. We

therefore compare our measurements to detection thresholds taken at the distal pad of the middle finger [32] and at the thenar eminence [31]. For both sets of data, we choose the threshold data taken with contactor areas that are closest to our experimental setup (0.3 cm^2 for finger tip and 1.3 cm^2 for thenar eminence). It turns out that the threshold curves from both body sites are quite similar at their respective chosen contact areas. Therefore, the detection thresholds from [31] at 1.3 cm^2 are used in our data analysis.

In the preliminary experiments, $p_z(t)$ showed the largest power spectral density among the three positional variables, as z direction is the normal vector of the underlying flat wall (see Fig. 2). We therefore compute the perceived magnitude in dB SL (sensation level) as the difference between the average spectral density of $p_z(t)$ and the detection threshold at the corresponding frequency.

For the stroking mode (Conditions D, E, F, and G), we estimate the location of the spectral peak corresponding to texture information, $\hat{f}_{tex}$, as follows:

$$\hat{f}_{tex} = \frac{\overline{|v_x|}}{L}, \tag{5}$$

where $\overline{|v_x|}$ is the average stroking velocity.

4 Experimental Results

As an example of the collected data, the experimental result for Condition D (stable stroking, Subject S1) are shown in Fig. 3, along with their power spectral densities. Note that the power spectral densities below 10 Hz are not shown because they are suspected to be 1/f noises [28]. The predicted location of the spectral component for texture information ($\hat{f}_{tex}$) is 50 Hz for this data set. As we expected, all the spectral densities in Fig. 3 show spectral peaks around 50-60 Hz. We therefore infer that the mechanical energy in this frequency band was responsible for the perception of desired virtual texture. It can be also observed that no prominent peaks appear at high frequencies for this condition. Furthermore, the locations of distinct peaks measured with three sensors are very consistent, except for the high-frequency noise in the accelerometer data caused by quantization error. This consistency across sensor measurements turned out to be true for all the experimental conditions. We therefore report only results obtained from the position data $p_z(t)$ in the rest of this paper.

For the experimental conditions employing the free exploration mode (Conditions A, B, and C), the power spectral densities of $p_z(t)$ exhibit dominant spectral peaks in the frequency range of 192-240 Hz. An example of such data (Condition C, Subject S2) is shown in Fig. 4(a). The upper panel is the spectral density function (solid line), along with the detection thresholds taken from [31] (filled triangles) and the linearly interpolated detection threshold curve (dotted line). The lower panel is the difference between the power spectral density and the detection threshold curve. The dotted line indicates the reference line for 0 dB SL. In both the upper and lower panels, a vertical solid line is drawn to locate the peak in the spectral density function. We observe that only the signal components around the spectral peaks are significantly above the absolute detection threshold. This fact is common to all experimental data for Conditions A, B, and C. It follows that the high-frequency spectral peaks observed in all these conditions are responsible for the perceived instability. This frequency is denoted by f_{ins}.

For each stroking data (Conditions D, E, F, and G), the predicted frequency $\hat{f}_{tex}$ of the spectral peak for texture perception (see Eqn. 5) is used to find the location of its corresponding actual spectral peak in the data (f_{tex}). Table 2 shows a close agreement between the values of $\hat{f}_{tex}$ and f_{tex}, with an average prediction error of 5.5 Hz. Recall that $\hat{f}_{tex}$

Table 2. Predicted and measured locations of the spectral peaks for texture perception.

Condition	Subject	$\hat{f}_{tex}$ (Hz)	f_{tex} (Hz)
D	S1	50	56
	S2	40	51
E	S1	39	41
	S2	29	26
F	S1	57	62
	S2	37	40
G	S1	56	65
	S2	21	26

Table 3. Intensities of spectral peaks (in sensation level) at frequencies for texture perception (f_{tex}) and perceived instability (f_{ins}). The sensation levels are in dB and the frequencies are in Hz.

Condition	Subject	SL @ f_{tex}	SL @ f_{ins}
A	S1	—	33.48 @ 221
	S2	—	39.31 @ 223
B	S1	—	33.01 @ 192
	S2	—	47.84 @ 238
C	S1	—	30.92 @ 205
	S2	—	48.79 @ 240
D	S1	8.91 @ 56	—
	S2	4.95 @ 51	—
E	S1	10.98 @ 41	25.57 @ 194
	S2	15.67 @ 26	25.89 @ 203
F	S1	13.83 @ 62	—
	S2	8.28 @ 40	—
G	S1	23.61 @ 65	26.53 @ 203
	S2	8.73 @ 26	21.21 @ 208

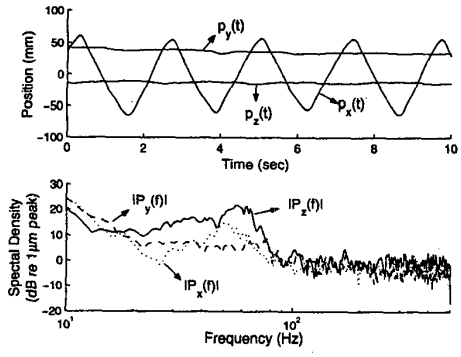

(a) Position

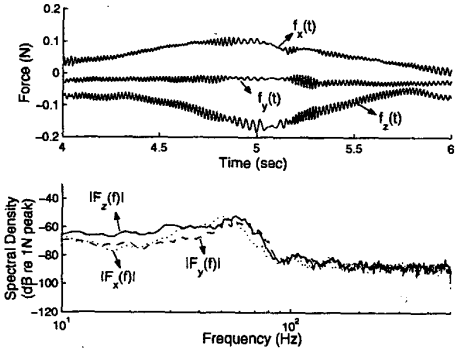

(b) Force

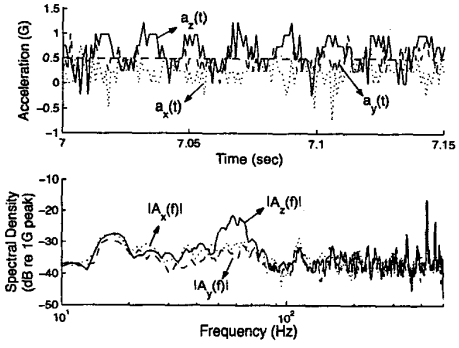

(c) Acceleration

Fig. 3. Experimental data for Condition D (Subject S1). The measured time-domain data are shown in the upper panels, and their power spectral densities in the lower panels.

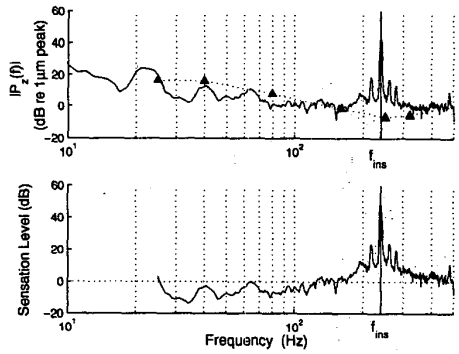

(a) Condition C, S2

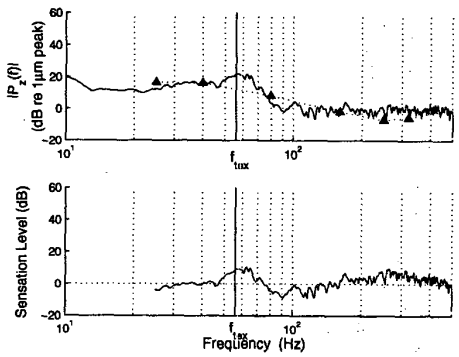

(b) Condition D, S1

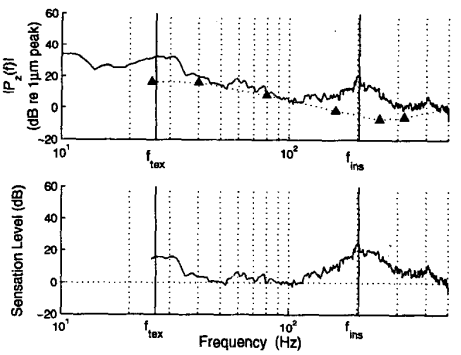

(c) Condition E, S2

Fig. 4. Average power spectral density of $p_z(t)$ and their corresponding sensation levels. The upper panels show the spectral densities (solid lines) with the detection thresholds at the thenar eminence (triangles). The lower panels show the sensation levels as the difference between spectral densities and detection thresholds.

is estimated under the assumption that the subject moved the stylus with a constant velocity. This may have been the main source of discrepancy between the predicted and measured values of f_{tex}.

An example of the stroking data for perceptually stable texture rendering is shown in Fig. 4(b) (Condition D, Subject S1). Only a spectral peak for texture perception at 56 Hz appears in this figure. Fig. 4(c) shows an example of the stroking data for perceptually unstable case (Condition E, Subject S2). It is evident that the spectral density function has prominent peaks (relative to detection thresholds) at two locations - one corresponding to the perception of textured surface, and the other to that of instability.

Finally, the sensation levels for spectral components at f_{tex} and f_{ins} are summarized in Table 3 for both subjects at every experimental condition. The average values of f_{tex} and f_{ins} are 45.9 and 213.7 Hz, respectively. Note that the range of f_{tex} (26-65 Hz) is well separated from that of f_{ins} (192-240 Hz).

5 Conclusions and Discussion

This study has investigated the sources of perceived instability associated with virtual textured surfaces rendered with a force-reflecting haptic interface. We have measured the time-series profiles of several physical variables (position, force and acceleration) at a stylus used by human observers for exploration of virtual textures. Based on our previous study [4], we have selected a range of experimental conditions differing in exploration mode, texture rendering method, and perceptual category. The recorded data are analyzed in the frequency domain. Signal intensities relative to human detection thresholds of sinusoidal motions at the corresponding frequencies are reported. We found that whenever a virtual textured surface is perceived to be unstable, there is a spectral peak in the measured signal in the intensity range of 21.21-48.79 dB SL over a frequency range of 192-240 Hz. For the stroking mode, we are able to predict, and then locate spectral peaks for texture perception in the recorded data. These lower frequency signal components, distributed in the frequency range of 26-65 Hz, are responsible for the perception of rendered textures. The two types of spectral components (26-65 Hz for texture and 192-240 Hz for instability) are well separated such that signals in these two frequency ranges are encoded by different mechanoreceptors (texture by Meissner and instability by Pacinian corpuscles [1]). They are therefore perceptually distinctive, and their sensory attributes are often described as "flutter" and "vibration," respectively [29].

At this point, we have established the parameter ranges for perceptually stable texture rendering [4], and characterized the signal components responsible for texture and instability perception (current study). We have yet to identify the mechanisms that give rise to the high-frequency "buzzing" responsible for perceived instability. Towards this end, a z-axis open-loop frequency response of the PHANToM is measured at the origin in the world coordinate frame. The result shows a mechanical resonance at 218 Hz. Similar resonance frequency has also been reported recently for model 1.5 of the PHANToM [2]. This resonance seems to be the source of the spectral peaks in the 192-240 Hz region that have appeared consistently in our measured data during perceptually unstable texture rendering. To investigate this issue further, we plan to fully identify the dynamics characteristics of our instrumented PHANToM in the near future.

Another issue that is under ongoing investigation is the effect of collision detection algorithms on the perceived stability. As shown in Eqn. 1, our algorithm calculates a rendering force when the stylus penetrates the underlying flat wall instead of the textured surface. This algorithm is commonly used due to its computational simplicity (especially when the underlying surface is more complicated than a flat plane), but introduces discontinuity in force magnitude. We have conducted psychophysical studies using a rendering algorithm that generates a force as soon as the stylus penetrates the sinusoidal gratings. This allows a smooth transition in the force magnitude when the stylus goes in and out of the textured surface. However, the generalization of this approach to a textured virtual object may not be as straightforward as that of the one used in this paper (in particular, on the edges), nor has this issue been seriously addressed in the literature. In this case, we have found that stiffness thresholds for stable texture rendering are higher under some experimental conditions, but comparable to those from our previous study under other conditions. In terms of the sensations associated with instability, we have found that subjects judged a textured surface as unstable when it seemed to be "alive" (i.e., actively pushing the tip of the stylus), or when "buzzing" was present. We plan to examine this percept of "aliveness" further by a measurement-based analysis similar to the one reported in this paper.

Acknowledgement

This work was supported in part by a National Science Foundation (NSF) Faculty Early Career Development (CAREER) Award under Grant 9984991-IIS, and in part by an NSF award under Grant 0098443-IIS. The comments from two anonymous reviewers are greatly appreciated.

References

[1] S. J. Bolanowski, Jr., G. A. Gesheider, R. T. Verrillo, and C. M. Checkosky. Four channels mediate the mechanical aspects of touch. *Journal of Acoustical Society of America*, 84(5):1680–1694, 1988.

[2] M. C. Cavusoglu, D. Feygin, and F. Tendick. A critical study of the mechanical and electrical properties of the PHANToM^{TM} haptic interface and improvements for high performance control. Submitted to *Presence*, 2001.

[3] S. Choi and H. Z. Tan. A parameter space for perceptually stable haptic texture rendering. In *Proceeding of the Fifth PHANToM Users Group Workshop*. 2000.

[4] S. Choi and H. Z. Tan. An analysis of perceptual instability during haptic texture rendering. To appear in *Proceedings of the Tenth Symposium on Haptic Interfaces for Virtual Environment and Teleoperator Systems* (in conjunction with IEEE VR 2002), 2002.

[5] C. E. Connor, S. S. Hsiao, J. R. Phillips, and K. O. Johnson. Tactile roughness: Neural codes that account for psychophysical magnitude estimates. *Journal of Neuroscience*, 10:3823–3836, 1990.

[6] C. E. Connor and K. O. Johnson. Neural coding of tactile texture: Comparison of spatial and temporal mechanisms for roughness perception. *Journal of Neuroscience*, 12:3414–3426, 1992.

[7] J. P. Fritz and K. E. Barner. Stochastic models for haptic texture. In *Proceedings of SPIE's International Symposium on Intelligent Systems and Advanced Manufacturing – Telemanipulator and Telepresence Technologies III*. Boston, MA, 1996.

[8] C. Ho, C. Basdogan, and M. A. Srinivasan. Efficient point-based rendering techniques for haptic display of virtual objects. *Presence*, 8(5):477–491, 1999.

[9] M. Hollins and S. R. Risner. Evidence for the duplex theory of tactile texture perception. *Perception & Psychophysics*, 62:695–705, 2000.

[10] K. O. Johnson and S. S. Hsiao. Neural mechanisms of tactual form and texture perception. *Annual Review of Neuroscience*, 15:227–250, 1992.

[11] K. O. Johnson and S. S. Hsiao. Evaluation of the relative roles of slowly and rapidly adapting afferent fibers in roughness perception. *Canadian Journal of Physiology & Pharmacology*, 72:488–497, 1994.

[12] D. Katz. *The World of Touch*. Lawrence Erlbaum Associates, Hillsdale, NJ, 1925/1989.

[13] R. L. Klatzky and S. J. Lederman. Tactile roughness perception with a rigid link interposed between skin and surface. *Perception & Psychophysics*, 61:591–607, 1999.

[14] R. L. Klatzky, S. J. Lederman, C. Hamilton, and G. Ramsay. Perceiving roughness via a rigid probe: Effects of exploration speed. In *Proceedings of the ASME Dynamic Systems and Control Division*, vol. 67, pp. 27–33. ASME, 1999.

[15] R. H. LaMotte and M. A. Srinivasan. Surface microgeometry: Tactile perception and neural encoding. In O. Franzen and J. Westman, editors, *Information Processing in the Somatosensory Systems, Wenner-Gren International Symposium Series*, pp. 49–58. MacMillan Press, 1991.

[16] S. J. Lederman. Tactual roughness perception: Spatial and temporal determinants. *Canadian Journal of Psychology*, 37:498–511, 1983.

[17] S. J. Lederman and R. L. Klatzky. Hand movement: A window into haptic object recognition. *Cognitive Psychology*, 19:342–368, 1987.

[18] S. J. Lederman and R. L. Klatzky. Feeling through a probe. In *Proceedings of the ASME Dynamic Systems and Control Division*, vol. 64, pp. 127–131. ASME, 1998.

[19] S. J. Lederman and R. L. Klatzky. Sensing and displaying spatially distributed fingertip forces in haptic interfaces for teleoperator and virtual environment systems. *Presence*, 8:86–103, 1999.

[20] S. J. Lederman, R. L. Klatzky, C. L. Hamilton, and G. I. Ramsay. Perceiving roughness via a rigid probe: Psychophysical effects of exploration speed and mode of touch. *Haptics-e (http://www.haptics-e.org)*, 1(1), 1999.

[21] S. J. Lederman, J. M. Loomis, and D. A. Williams. The role of vibration in the tactual perception of roughness. *Perception & Psychophysics*, 32:109–116, 1982.

[22] S. J. Lederman and M. M. Taylor. Fingertip force, surface geometry, and the perception of roughness by active touch. *Perception & Psychophysics*, 12:401–408, 1972.

[23] T. H. Massie. Initial haptic explorations with the phantom: Virtual touch through point interaction. Master's thesis, MIT, Feb. 1996.

[24] M. Minsky and S. J. Lederman. Simulated haptic textures: Roughness. In *Proceedings of the ASME Dynamic Systems and Control Division*, vol. 58, pp. 421–426. ASME, 1996.

[25] M. D. R. Minsky. *Computational Haptics: The Sandpaper System for Synthesizing Texture for a Force-Feedback Display*. PhD thesis, MIT, June 1995.

[26] D. Ruspini, K. Kolarov, and O. Khatib. The haptic display of complex graphical environments. In *Computer Graphics Proceedings, Annual Conference Series*, pp. 345–352. ACM SIGGRAPH 97, 1997.

[27] J. Siira and D. K. Pai. Haptic texturing - a stochastic approach. In *Proceedings of the IEEE International Conference on Robotics and Automation*, pp. 557–562, 1996.

[28] S. W. Smith. *The Scientist and Engineer's Guide to Digital Signal Processing*. California Technical Publishing, P.O. Box 502407 San Diego, CA 92150-2407, second edition, 1999.

[29] H. Z. Tan, N. I. Durlach, C. M. Reed, and W. M. Rabinowitz. Information transmission with a multifinger tactual display. *Perception & Psychophysics*, 61(6):993 – 1008, 1999.

[30] M. M. Taylor and S. J. Lederman. Tactile roughness of grooved surfaces: A model and the effect of friction. *Perception & Psychophysics*, 17:23–36, 1975.

[31] R. T. Verrillo. Effect of contactor area on the vibrotactile threshold. *The Journal of the Acoustical Society of America*, 35(13):1962–1966, 1963.

[32] R. T. Verrillo. Vibrotactile thresholds measured at the finger. *Perception & Psychophysics*, 9(4):329–339, 1971.

[33] S. A. Wall and W. S. Harwin. Modeling of surface identifying characteristics using Fourier series. In *Proceedings of the ASME dynamic systems and control division*, vol. 67, pp. 65–71, 1999.

[34] S. A. Wall and W. S. Harwin. Effects of physical bandwidth on perception of virtual gratings. In *Proceedings of the ASME Dynamic Systems and Control Division*, vol. 69, pp. 1033–1039, 2000.

[35] J. M. Weisenberger, M. J. Krier, and M. A. Rinker. Judging the orientation of sinusoidal and square-wave virtual gratings presented via 2-DOF and 3-DOF haptic interfaces. *Haptics-e (http://www.haptics-e.org)*, 1(4), 2000.